Journal of Microscopy, Vol. 202, Pt 1, April 2001, pp. 142–147.
Received 28 August 2000; accepted 1 December 2000

Fundamental differences between micro- and nano-Raman spectroscopy

E. J. AYARS,[1] C. L. JAHNCKE†, M. A. PAESLER* & H. D. HALLEN*
**Physics Department, North Carolina State University, Raleigh, NC 27695-8202, U.S.A.*
†Physics Department, St. Lawrence University, Canton, NY 13617, U.S.A.

Key words. Infra-red spectroscopy, near-field optical microscopy, Raman spectroscopy.

Summary

Electric field polarization orientations and gradients close to near-field scanning optical microscope (NSOM) probes render nano-Raman fundamentally different from micro-Raman spectroscopy. With *x*-polarized light incident through an NSOM aperture, transmitted light has *x*, *y* and *z* components allowing nano-Raman investigators to probe a variety of polarization configurations. In addition, the strong field gradients in the near-field of a NSOM probe lead to a breakdown of the assumption of micro-Raman spectroscopy that the field is constant over molecular dimensions. Thus, for nano-Raman spectroscopy with an NSOM, selection rules allow for the detection of active modes with intensity dependent on the field gradient. These modes can have similar activity as infra-red absorption modes. The mechanism can also explain the origin and intensity of some Raman modes observed in surface enhanced Raman spectroscopy.

Introduction

When micro-Raman spectroscopy became a viable technique, there was some question as to whether there were fundamental differences between it and conventional Raman spectroscopy (Delhaye & Dhamelincourt, 1975; Rosasco *et al.*, 1975). As it turned out, the introduction of a microscope objective in micro-Raman spectroscopy introduced no fundamental changes in the technique. Thus, micro-Raman is now viewed as a conventional Raman technique simply with enhanced resolution that is bounded by the far-field diffraction limit.

As near-field techniques have matured, spectral analysis coupled with nanometric resolution has become a reality (Paesler & Moyer, 1996) and a new question has emerged: are there fundamental differences between micro- and nano-Raman spectroscopy? This time the question is answered resoundingly in the affirmative. There are fundamental differences that lead to new capabilities and new interpretations of Raman data.

The electric field in the vicinity of an near-field optical scanning microscope (NSOM) probe is distinct in three very important ways from the field of a spot focused as tightly as possible on a small region of space. First, in the near-field, evanescent fields contribute considerably and intensities are often much stronger than those that can be obtained in conventional far-field configurations. In NSOM, the majority of this enhanced intensity is localized to a region directly in front of the aperture. As this region is normally obscured from the collection optics in reflection-mode nano-Raman configurations, this difference is of little consequence. Second, for *x*-polarized light passing towards the NSOM probe, light with *x*-, *y*- *and z* components will be present in a small sample volume near the output of the probe. This allows for excitation of a variety of modes without requiring reorientation of the sample. A third effect in nano-Raman spectroscopy results from the strong electric field gradients in the vicinity of the NSOM probe. In the standard derivation of the Raman effect, one assumes a constant electric field. Even for confocal Raman spectroscopy, this is an excellent approximation; the electric field intensity does not change measurably over molecular distances. In nano-Raman spectroscopy, by contrast, the presence of a non-negligible field gradient affects the measurement in a fundamental way.

In the following section, Raman spectroscopy is briefly outlined to give a framework for the following two sections on polarization and gradient effects. Then, following a brief section on experimental design, results of nano-Raman measurements provide demonstrations of both the polarization and the gradient field effects.

Correspondence to: M. Paesler. Tel.: + 1 919 515 8706; fax: +1 919 515 3031; e-mail: paesler@ncsu.edu

[1]Present address: Physics Department, Walla Walla College, College Place, WA 99324, U.S.A.

Raman spectroscopy

The polarization P of the material depends on the polarizability α of the material and on the electric field E of the incident light at frequency ν_0 (Ferraro & Nakamoto, 1994).

$$P = \alpha E_0 \cos(2\pi \upsilon_0 t).$$

Charges in the material may oscillate at some frequency ν_m about their equilibrium positions:

$$q = q_0 \cos(2\pi \upsilon_m t).$$

Usually the electric field magnitude E_0 is presumed to be constant over the dimensions of the oscillations. This is an excellent approximation for visible light in far-field configurations. The oscillations may, however, induce a change in the polarizability of the material, which can be approximated by a Taylor expansion of α:

$$\alpha = \alpha_0 + \left(\frac{\partial \alpha}{\partial q}\right)_0 q + O(q^2).$$

Combining these and simplifying gives, to first order in q,

$$P = \alpha_0 E_0 \cos(2\pi \upsilon_0 t) + \tfrac{1}{2} q_0 \left(\frac{\partial \alpha}{\partial q}\right)_0 E_0[\cos\{2\pi(\upsilon_0 - \upsilon_m)t\} + \cos\{2\pi(\upsilon_0 + \upsilon_m)t\}] + O(q^2)$$

The first of these terms is the Rayleigh scattering, and the second is the Raman scattering. The existence of Raman-scattered light depends on the Raman activity $\delta\alpha/\delta q$. If there is no change in the polarizability for a given vibrational transition then $\delta\alpha/\delta q = 0$ and the transition is not Raman-active. In three dimensions, change in the polarizability tensor determines the activity, and the vibration is Raman-active if any one of the polarizability tensor components is changed during the vibration.

Polarization effects

Whether one appeals to the more idealistic analytical results of Bethe (1944) and Bouwkamp (1950) or any of the more recent realistic numerical work such as that of Martin (1999), theoretical work suggests that with x-polarized light incident on an aperture, the transmitted light has x, y and z components. The total intensity of the transmitted radiation varies strongly with distance from the tip, as do each of the components.

In conventional normal incidence Raman spectroscopy, vibrational modes with x or y components are excited by the incident light, which is necessarily polarized in the xy plane. Modes with purely z components require an electric field in the z direction for excitation. The z modes are usually measured by reorienting the crystal so that the incident light has a polarization component along the desired axis. In near-field Raman, there is a z component of the field which provides excitation of these modes without reorientation of the crystal. Theoretical studies show that the integrated z polarization intensity in the very near field is actually stronger than the total field in the far-field.

Field gradient effects

Classically, the effect of the field gradient can be explored by taking a Taylor expansion of the electric field

$$E = E_0 + \left(\frac{\partial E}{\partial q}\right)_0 q + O(q^2)$$

and including it in the above derivation. This results in a polarization given by

$$P = \alpha_0 E_0 \cos(2\pi \upsilon_0 t) + \tfrac{1}{2} q_0 \left(\frac{\partial \alpha}{\partial q}\right)_0 E_0[\cos\{2\pi(\upsilon_0 - \upsilon_m)t\} + \cos\{2\pi(\upsilon_0 + \upsilon_m)t\}] + \tfrac{1}{2} q_0 \left(\frac{\partial E}{\partial q}\right)_0 \alpha_0[\cos\{2\pi(\upsilon_0 - \upsilon_m)t\} + \cos\{2\pi(\upsilon_0 + \upsilon_m)t\}] + O(q^2)$$

The first two terms are the same as before. The third describes a scattering with the Stokes and anti-Stokes frequency shifts similar to the Raman lines. Instead of a dependence on activity $\delta\alpha/\delta q$, however, this scattering term is dependent on the field gradient and the polarizability. Selection rules for this term depend on the characteristics of α, and so would have similar activity as IR absorption spectroscopy. This is the gradient field Raman, or GFR, term.

An identical result follows quantum mechanically. In this case, transitions in vibration levels due to coupling with a radiation field are described by the perturbation Hamiltonian:

$$H = \mu \cdot \mathrm{E}$$

where $\boldsymbol{\mu}$ is the dipole moment and E is the electric field. The electric dipole moment can be written as

$$\mu_\alpha = \mu_\alpha^p + \alpha_{ab} E_b + \tfrac{1}{3} A_{abc} \frac{\partial E_b}{\partial c} + \ldots$$

where the $\{a,b,c\}$ are a permutation of the coordinates $\{x,y,z\}$ and summing over repeated indices is implied. B is the magnetic field; α and A are given by: (Sass *et al.*, 1981)

$$\alpha_{ab} = \frac{1}{\hbar} \sum_j H(\omega) \langle i | \mu_\alpha^p | j \times j | \mu_b^p | f \rangle$$

where $H(\omega) = \omega_{ji}/({\omega_{ji}}^2 - \omega^2)$; and where μ^p and θ, m are the permanent electric dipole and the quadrupole operator, respectively, and and are the initial and final states of the system, respectively.

The derivation of the spectroscopic signals originates with a first-order expansion of μ in the coordinate of vibration q. Terms without q dependence may be discarded because they will not couple adjacent vibration states. Upon removal of high order terms that are small even in the case of large field gradients, the relevant dipole terms can be written as:

$$\mu_a = \left[\left(\frac{\partial \mu_a^p}{\partial q}\right)_0 + \left(\frac{\partial \alpha_{ab}}{\partial q}\right)_0 E_b + \left(\frac{\partial E_b}{\partial q}\right)_0 \alpha_{ab} + \frac{1}{3}\frac{\partial E_b}{\partial c}\left(\frac{\partial A_{abc}}{\partial q}\right)_0\right] q$$

These four terms result in IR absorption, Raman, gradient field Raman (GFR), and quadrupole-Raman, respectively.

The ratio of the GFR term to the Raman term depends upon the field gradient and the polarizability gradient. We approximate the polarizability gradient by α/a, where a is close to an atomic dimension. This gives us a ratio of GFR to Raman of:

$$\frac{G}{R} \approx \frac{\alpha}{E}\frac{\partial E}{\partial q}$$

In vacuum, the field gradient yields terms of the order $(2\pi/\lambda)E_b$. The ratio of the GFR term to the Raman term is then (for 500 nm light and $a = 0.2$ nm)

$$\frac{G}{R} \approx \frac{a}{E}\left(\frac{2\pi}{\lambda}E\right) = \frac{2\pi a}{\lambda} \approx 3 \times 10^{-3}$$

Thus, any GFR contribution is insignificant in vacuum.

Near a metal surface, the jellium approximation (Feibelman, 1975) indicates that the normal component of the electric field varies by nearly its full amplitude over a distance of 0.2 nm. The field gradient is then approximately E_b/0.2 nm, and

$$\frac{G}{R} \approx \frac{a}{E}\left(\frac{E}{0.2nm}\right) \approx 1$$

One could thus expect to find a measurable GFR signal near metal surfaces.

The GFR differs appreciably from Raman spectroscopy in selection rules. These rules result from the requirement that $\langle\psi_f|\,\mu\cdot E\,|\psi_i\rangle$ be non-zero. The q dependence of $\boldsymbol{\mu}$ means that this expectation will be non-zero if the ψ differ by one vibrational quantum. In addition, the coefficient of q must be non-zero. The Raman selection rules are determined by the requirement

$$\left(\frac{\partial \alpha}{\partial q}\right)_{q=0} \neq 0$$

This is equivalent to the condition that α and the vibration belong to the same symmetry species (Ferraro & Nakamoto, 1994). Conversely, the GFR selection rules require that E belong to the same symmetry species as the vibration, or

$$\left(\frac{\partial \mathbf{E}}{\partial q}\right)_{q=0} \neq 0$$

This will be true if the vibration has a component normal to the surface, as that is the direction in which E varies most rapidly. The polarizability must also be non-zero. For example, if z is normal to the surface, then α_{az} and E_a must be non-zero. This is the case for NSOM, in which the largest components of E are near the probe (Betzig & Trautman, 1992), but it is certainly not the case in far-field measurements. The GFR effect should scale with polarizability, and should thus be stronger for ionic systems. This is in contrast to Raman spectroscopy, which typically is stronger for covalent bonding. The GFR effects should also be strongest for the vibration modes for which infrared absorption is strong. That is, the GFR spectra will complement the Raman spectra in many materials, particularly centro-symmetric materials. The extra requirement for observation of the GFR effect is a strong field gradient along the vibrating bond.

The effects of a strong electric field gradient on Raman spectra has been discussed previously as a mechanism for some of the observed spectral lines in SERS (Sass *et al.*, 1981). As there is no good, controllable method of regulating distance or field gradient in SERS, NSOM-Raman offers the first opportunity to test the distance dependence of this effect. The GFR effect was also predicted as an effect in the Raman spectra of microparticles suspended in laser traps (Knoll *et al.*, 1988).

Experimental set-up

Aluminium-coated etched fibre tips were positioned near the surface of samples under investigation, and spectra were taken with the tip near the surface under lateral force feedback. The NSOM was used in the illumination mode with 514 nm laser light. Reflected light is collimated with a 0.50 NA lens and is passed through a holographic filter, focused into a single stage 1 m spectrometer with a resolution of 3 cm^{-1}, and collected onto a cooled CCD camera. Light reflected from the filter is simultaneously gathered to provide a reflection image and to verify that observed effects are not attributable to laser power fluctuations.

The tip mounting assembly eliminates problems associated with high mechanical Q and allows for large collection efficiency, see Fig. 1. By gluing one leg of the tuning fork to the base, the symmetry of the oscillator is destroyed and the resonator changes from a low-loss tuning fork to a high-loss vibrating beam with a resonance of 35–37 kHz. With one arm of the fork fixed, higher level harmonics in the fork do not cancel and are used for feedback. At the second cantilever beam mode around

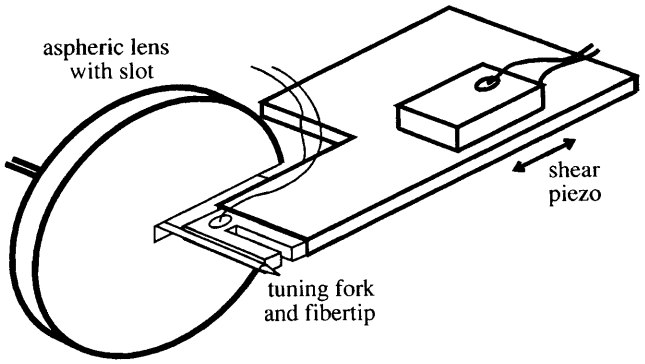

Fig. 1. NSOM tip-holder assembly and collection optic. The holder is a 1-inch long conventional microscope cover slide. The tuning fork is glued to the end of the holder. A slot is cut in the aspheric lens to accommodate the fork and tip.

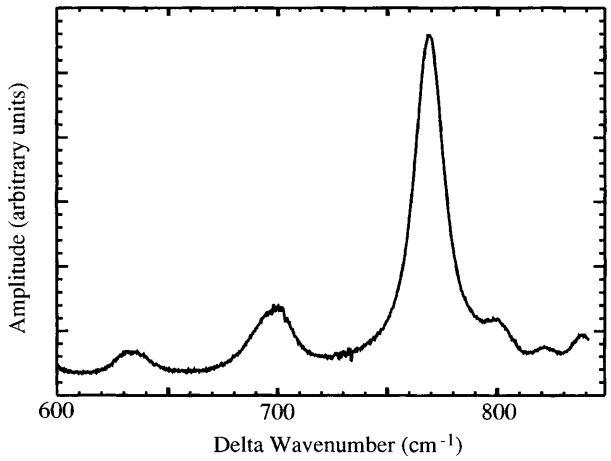

Fig. 2. Typical KTP Raman spectrum. This spectrum with 3 cm^{-1} resolution was taken with the NSOM configured as shown in Fig. 1. Spectrum obtained in approximately 5 min.

90 kHz the Q is reduced by a factor of 10 and the mechanical limit on bandwidth is reduced by a factor of 30 or more. Scanning of the sample is accomplished with a standard four-quadrant piezo tube, and the coarse approach mainframe consists of a monolithic double-compound flexure. The collection optics, scan tube/sample holder, and tip mount are all affixed to the flexure which is firmly mounted inside a copper thermal isolation box. The material studied is $KTiOPO_4$ (KTP), a nonlinear optical material used for second harmonic generation.

Results and discussion

A Raman spectrum taken with the tip held in the far-field of the sample is shown in Fig. 2, where uncertainty in the abscissa is 0.5 cm^{-1}. The 767 cm^{-1} peak is the symmetric A1 vibration reported in both near- and far-field measurements (Kugel *et al.*, 1988; Jahncke *et al.*, 1995). Features at 698 cm^{-1} and at 631 cm^{-1} can be identified as an A2 vibration and a weaker A1 vibration, respectively. The shoulder at roughly 800 cm^{-1} could be associated with a vibration at 789 cm^{-1} reported by Yang *et al.* (1986).

As the tip is brought into the near-field of the sample, the features change subtly. Difference spectra allow one to focus on the changes in the spectrum as the near-field effects come into play. Thus, a series of spectra was obtained as the tip approached the sample, and each spectrum was subtracted from a far-field NSOM spectrum such as that of

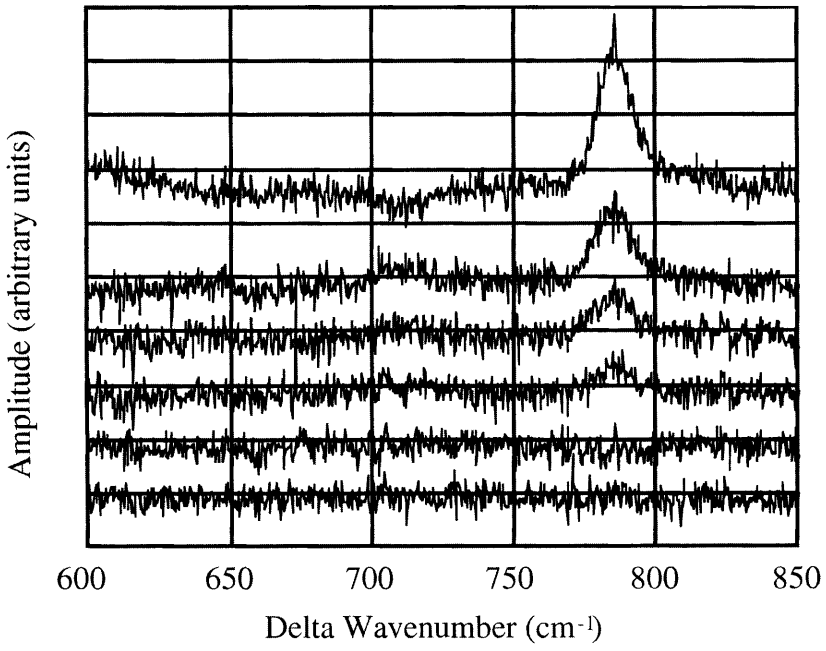

Fig. 3. KTP difference spectra at varying near-field distances. Spectra represent the difference between the spectra taken and the spectrum taken with the tip retracted to the far-field as in Fig. 2. Reading from the top to the bottom, the distances are: (a) in contact with the surface, (b) just out of contact, (c) 47 nm further than (b), (d) 70 nm further than (b), (e) 108 nm further than (b), and (f) 127 nm further than (b). Spectra were obtained in approximately 5 min, and distances are accurate to 0.5 nm.

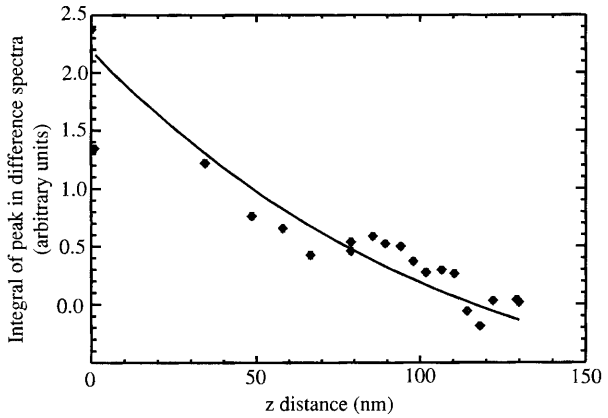

Fig. 4. Integral of the area under the 785 cm^{-1} peak vs. distance between the sample and the tip. The solid line represents a numerical integration of the Bethe–Boukamp model of the z component of the electric field.

Fig. 2. Spectra took approximately 5 min to obtain. These difference spectra are shown in Fig. 3. From the top to the bottom, the spectra correspond to the following positions to within 0.5 nm: (a) in contact with the surface, (b) just out of contact, (c) 47 nm further than (b), (d) 70 nm further than (b), (e) 108 nm further than (b), and (f) 127 nm further than (b). Reading from bottom to top, it is clear that a large feature at 785 cm^{-1} appears as the tip is brought into the near-field of the sample. This peak can be identified as that reported by Yang *et al.* (1986) at 783 cm^{-1}, which posseses B1 symmetry. The B1 symmetry requires a polarization component in the z-direction, normal to the surface. The data of Fig. 3 thus provide a demonstration of the fact that varying polarization states may be sampled in an NSOM Raman experiment merely by adjusting the distance between the tip and the sample. This capability is unique to nano-Raman spectroscopy.

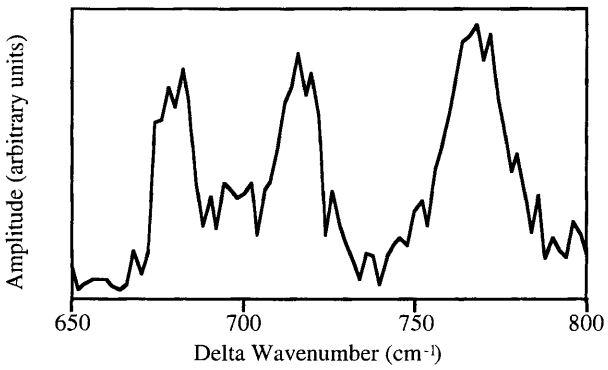

Fig. 5. A nano-Raman scan of KTP with the tip in the near-field of the sample. The peaks at 683, 695, and 676 cm^{-1} are identifiable Raman peaks. The peak at 712 cm^{-1} is not explained by conventional Raman or z-polarization effects. It may be identified as an IR active mode excited by the large electric field gradient inherent in nano-Raman spectroscopy performed with an NSOM.

As further evidence that the feature at 785 cm^{-1} is indeed a z-sensitive Raman mode, the distance dependence of this feature is plotted in Fig. 4. Also shown is the distance dependence of the squared z component of the electric field as calculated by the Bethe-Bouwkamp model (Bouwkamp, 1950). Several numerical models of the near-field of an NSOM tip may provide more realistic estimates of the field strength, but the Bethe–Bouwkamp result is analytically accessible and is qualitatively indistinguishable from other models. One arbitrary scale factor is used to shift the data along the ordinate. This scaling is equivalent to assuming a certain aperture size. The single point on the ordinate represents the contact spectrum. Its coordinate on the abscissa is somewhat arbitrary, as the tip flexes on contact. Agreement between the data and the theoretical fit of Fig. 4 suggest that the 785 cm^{-1} mode is indeed attributable to a z-sensitive Raman mode. In these NSOM nano-Raman spectra, therefore, clear sensitivity to z-polarization Raman activity is evident. Similar fall-off of Raman signal with distance in an NSOM has been reported elsewhere (Jordan *et al.*, 1999).

In a spectrum taken over several hours in a similar NSOM configuration, a peak emerges than cannot be attributed to a Raman active mode of any orientation, including z-polarization. This peak appears at 712 cm^{-1}, as can be seen in Fig. 5. In this raw (unfiltered non-difference) spectrum, several Raman peaks can be identified. The left peak at 683 cm^{-1} is a B1 vibrational mode. The hump at 695 cm^{-1} is the A2 vibration, and the familiar peak at 676 cm^{-1} is the A2 symmetrical vibration. The peak at 712 cm^{-1} is not explained by conventional Raman or z-polarization effects. Once again, the distance dependence of the peak is instructional. In Fig. 6, the near-field enhancement of the 712 cm^{-1} peak is plotted as a function of distance. According to the theory developed above, if the peak does indeed represent the GFR effect, its height should scale with the magnitude of the z component of the electric

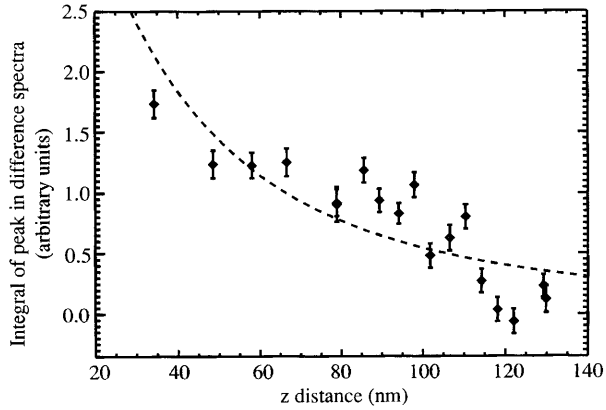

Fig. 6. Near-field enhancement of the 712 cm^{-1} peak. The dashed line represents a fit to the magnitude of the z component of the electric field times the gradient of that field.

field times its gradient. This dependence is shown as the dashed line in the figure. Given the noise in the data, the fit can be said to be semi-quantitatively correct. The peak may therefore be identified as the well known IR active mode at 712 cm^{-1}. It is rendered observable in this Raman spectrum by the presence of the large electric field gradient in the near-field of the NSOM probe.

Conclusion

Nano-Raman spectroscopy is fundamentally different from micro-Raman spectroscopy. In NSOM-based nano-Raman experiments, alternative polarization states may be sampled by adjusting the tip–sample spacing. In particular, *z*-polarization active modes become observable when the tip is in the near-field of a sample surface (in the *x*-*y* plane) that is illuminated through a probe excited with *x*-polarized light. Also, IR active modes can be observed in nano-Raman spectroscopy because of the large field gradients in the near-field of an NSOM probe.

Acknowledgements

The authors acknowledge discussions with Edgar Etz and Wolfgang Kiefer. The help of Bev Clark and Greg McDowall in developing our tip-etching technology is gratefully acknowledged. Work was supported by the US Army Research Office through grant DAAH04-97-1-0333, and the National Science Foundation through grant DMR-9731815.

References

Bethe, H. (1944) Theory of diffraction by small holes. *Phys Rev.* **66**, 163–182.

Betzig, E. & Trautman, J.K. (1992) Near-field optics: microscopy, spectroscopy, and surface modification beyond the diffraction limit. *Science*, **257**, 189–195.

Bouwkamp, C.J. (1950) On the diffraction of electromagnetic waves by small circular discs and holes. *Philips Res. Report*, **5**, 401–422.

Delhaye, M. & Dhamelincourt, P. (1975) Raman microprobe and microscope with laser excitation. *J. Raman Spectroscopy*, **3**, 33–43.

Feibelman, P.J. (1975). *Phys. Rev. B*, **12**, 1319.

Ferraro, J. & Nakamoto, K. (1994) *Introductory Raman Spectroscopy*. Academic Press, Inc., New York.

Jahncke, C.L., Paesler, M.A. & Hallen, H.D. (1995) Raman imaging with near-field scanning optical microscopy. *Appl. Phys. Lett.* **67**, 2483–2485.

Jordan, C.E., Stranick, S.J., Cavanagh, R.R., Richter, L.J. & Chase, D.B. (1999) Near-field scanning optical microscopy incorporating Raman scattering for vibrational mode contrast. *Surf. Sci.* **433–435**, 48–52.

Knoll, P., Marchi, M. & Kiefer, W. (1988) Raman spectrsocopy of microparticles in laser light traps. *Indian J. Pure Appl. Phys.* **26**, 268–277.

Kugel, G.E., Bréhat, F., Wyncke, B., Fontana, M.D., Marnier, G., Carabatos-Nedelec, C. & Mangin, J. (1988) The vibrational spectrum of a $KTiOPO_4$ single crystal studied by Raman and infrared reflectivity spectrsocopy. *J. Phys. C: Solid State Phys.* **21**, 5565–5583.

Martin, O.J.F. (1999) 3D simulations of the experimental signal measured in a near-field optical microscope. *J. Microsc.* **194**, 235–239.

Paesler, M.A. & Moyer, P.J. (1996) *Near-Field Optics: Theory, Instrumentation, and Applications*. John Wiley & Sons, Inc, New York.

Rosasco, G.J., Etz, E.S. & Cassatt, W.A. (1975) The analysis of discrete fine particles by Raman spectroscopy. *Appl. Spectroscopy*, **29**, 396–404.

Sass, J.K., Neff, H., Moskovits, M. & Holloway, S. (1981) Electric field gradient effects on the spectroscoy of adsorbed molecules. *J. Phys. Chem.* **85**, 621–623.

Yang, H., Gu, B., Wang, Y., Huang, C. & Shen (1986) Polarized Raman spectra of single crystal potassium titanium oxide phosphate ($KTiOPO_4$). *Guangxue Xuebao*, **6**, 1071–1080.